Nuclear Multicatalytic Proteinase α Subunit RRC3: Differential Size, Tyrosine Phosphorylation, and Susceptibility to Antisense Oligonucleotide Treatment†

Catharine M. Benedict, Ling Ren, and Gary A. Clawson*

Departments of Pathology, Biochemistry and Molecular Biology, and Cell and Molecular Biology Program, The Pennsylvania State University, Hershey, Pennsylvania 17033

Received February 3, 1995; Revised Manuscript Received April 25, 1995®

ABSTRACT: Multicatalytic proteinases (MCPs) are macromolecular structures involved in intracellular degradation of many types of proteins. MCPs are composed of a 20S "core" which consists of both structural (α) and presumed catalytic (β) subunits in association with complexes of accessory proteins. Immunohistochemical studies have shown MCP subunits to be largely cytoplasmic, although nuclear localization is also observed. Reverse transcription/polymerase chain reaction amplifications were performed with redundant primers to conserved regions within known subunits, in an attempt both to identify potential new subunits and to define the repertoire of subunits expressed in hepatocytes. No new subunits were identified, and we found that RRC3, an α subunit of MCPs which contains a putative nuclear localization signal (NLS), was the predominant α subunit expressed in hepatocytes and hepatocyte-derived cell lines. Antibodies were developed against a unique C-terminal peptide region of RRC3. Immunohistochemical studies using affinity-purified antibodies showed that RRC3 has both cytoplasmic and nuclear localizations. Immunoprecipitation/immunoblot analyses showed that a significant proportion of nuclear RRC3 was associated with the nuclear scaffold (NS). NS RRC3 showed a significantly smaller M_r (24 000) than the cytoplasmic form (M_r 28 000), and only the nuclear form contained phosphotyrosine. In metabolic labeling experiments with [^{32}P]orthophosphate, the major nuclear and NS form observed showed an M_r of 24 000, whereas no labeling of cytosolic RRC3 was observed. A minor ^{32}P-labeled band of M_r 28 000 was also observed in nuclei, and this M_r 28 000 form was found in the soluble nuclear extract within MCP complexes. These results suggest that tyrosine phosphorylation of the cytosolic form (M_r 28 000) rapidly triggers nuclear import, which is in turn quickly followed by conversion to the major M_r 24 000 form associated with NS. Treatment with antisense oligonucleotides targeted to the initiation site of RRC3 reduced the growth of a hepatocyte-derived cell line by 95% and produced a marked morphological change (in the absence of overt toxicity). Under these treatment conditions, RRC3 mRNA was dramatically reduced. RRC3 protein was also dramatically reduced in the NS, but showed only a small reduction in cytosol, suggesting that the nuclear RRC3 may be important in cell growth and differentiation.

The nuclear scaffold (NS)[1] includes an orthogonal array f intermediate filaments (Aebi et al., 1986), termed lamins, /hich serve to anchor chromatin (Newport & Forbes, 1987; :enta et al., 1991) as well as furnish a superstructure for a ariety of processes such as RNA editing (Carter et al., 1993; .awrence et al., 1989; Xing et al., 1993). We have reviously noted that a subset of lamins A/C is proteolytically leaved to produce an M_r 46 000 ATP-binding protein, which ıay function as an NTPase for nucleocytoplasmic RNA ·ansport (Clawson et al., 1990). Since this cleavage removes ıe nuclear localization signal (NLS) from lamins, we xamined NS for proteolytic activity. A Ca^{2+}-dependent diisopropyl fluorophosphate (DFP)-inhibitable protease (NS protease) capable of cleaving lamins A/C was identified (Clawson et al., 1990, 1992; Madsen et al., 1990; Tokes & Clawson, 1989), which exhibits both chymotrypsin- and trypsin-like substrate specificities (Clawson et al., 1992). These properties [and others such as stimulation by poly(L-lysine)] suggest that the NS protease represents a multicatalytic proteinase (MCP). The size (a closely spaced doublet of M_r 29 000) of the catalytic subunits of the NS protease [labeled with [^{3}H]DFP; see Clawson et al. (1992)] is consistent with those of MCP subunits, which have M_rs of 21 000−35 000.

MCPs are macromolecular structures that are generally isolated as large cytoplasmic complexes of 26S (Hershko & Ciechanover, 1992; Hough et al., 1987) with an M_r of 2×10^6 (Peters et al., 1994). Further "purification" techniques remove a significant number of higher M_r components, yielding a 20S MCP "core" (Hough et al., 1987) containing several different subunit proteins (M_r 21 000−35 000). The higher M_r proteins presumably represent regulatory factors; their removal is often associated with loss of ATP dependence (Hough et al., 1987; Tsukhara et al., 1988) or Ca^{2+} dependence (Dahlmann et al., 1989). Indeed, the regulatory

† This work was supported by grants from the National Institutes of [ealth (CA21141, CA40145).

* Correspondence should be addressed to this author at the Depart-ıent of Pathology, The Hershey Medical Center, P.O. Box 850, [ershey, PA 17033. Phone: (717) 531-5632. Fax: (717) 531-5298.

® Abstract published in *Advance ACS Abstracts,* July 15, 1995.

[1] Abbreviations: NS, nuclear scaffold; MCP, multicatalytic protein-se; NLS, nuclear localization signal; DFP, diisopropyl fluorophosphate; 'DM, chemically defined medium; FCS, fetal calf serum; RT, reverse ·anscription; PCR, polymerase chain reaction; DTT, dithiothreitol; .MC, 7-amino-4-methylcoumarin; $_{ms}$AAPF$_{sb}$, methoxysuccinyl-AAPF--benzyl.

0006-2960/95/0434-9587$09.00/0

factors themselves can be complex structures, such as the 11S "regulator" and 20S "ATPase complex" which appear to modulate MCP function (Hoffman & Rechsteiner, 1994).

The prototypical structure of the MCP is based on studies of the archeabacterium *Thermoplasma acidophilum*, in which MCPs are composed of multiple copies of only two different peptides, denoted α and β (Puhler et al., 1992). The α subunits are thought to represent structural or regulatory subunits, whereas the β subunits represent the presumed catalytic subunits, although both α and β subunits can be labeled with DFP at relatively high concentrations (Dahlmann et al., 1992). The cloning of homologs from a wide variety of species (including human, rat, yeast, and *Drosophila*) indicates that MCP subunits are related to either the α or the β prototype, defining two distinct families of MCP subunits (Bey et al., 1993; Heinemeyer et al., 1994). In eukaryotes, there appear to be 7α and 7β subgroups (Heinemeyer et al., 1994); in rat, 13 subunits have been sequenced, 6 of which are α and 7 of which are β. The structure of the prototypical 20S MCP is that of a barrel composed of four rings, each consisting of seven subunits; the outermost rings contain α subunits, and the two innermost rings consist of β subunits (Puhler et al., 1992). Different α and β subunits are presumably intermixed in eukaryotic MCP rings, and there is some evidence to suggest that the rings contain six subunits (Rechsteiner et al., 1993). Also of interest is the fact that the α subunit of *Thermoplasma acidophilum* contains a consensus NLS, which is located peripherally in the outer ring (Zwickl et al., 1992).

MCP complexes appear to have a wide variety of functions, including involvement in degradation of abnormally folded proteins and in the breakdown of proteins with very rapid turnover rates. MCP proteolysis can be ubiquitin-dependent, as in the *in vitro* destruction of cyclins (Glotzer et al., 1991; Seufert et al., 1995; Treier et al., 1994; Richter-Ruoff & Wolf, 1993) and several nuclear oncoproteins (Scheffner et al., 1993; Ciechanover et al., 1991), or ubiquitin-independent, as is seen *in vivo* with the breakdown of ornithine decarboxylase (Sheetz & Tager, 1988), and has been implicated in cell cycle control (Ghislain et al., 1993; Gordon et al., 1993). MCPs also appear to be involved in class I antigen presentation. The mouse MCP subunits LMP2 and LMP7 (Driscoll et al., 1993) or the human MCP subunits Ring 10 and Ring 12 (Glynne et al., 1991; Kelley et al., 1991) lie within the major histocompatibility complex class II region: these subunits play a role in regulation of MCP activity (Fruh et al., 1994). Certain β subunits appear to be associated with specific activities of the MCPs. For instance, PRE4 (from yeast) is necessary for peptidylglutamyl peptide hydrolase activity (Hilt et al., 1993), Ring 10 (the human homolog of RRC1 in rat) appears to be essential for chymotrypsin-like activity of MCPs (Heinemeyer et al., 1993), and Ca^{2+} differentially affects proteolytic activities vs cleavage of peptide substrates (Dahlmann et al., 1992). Finally, many MCP subunits are essential for cell viability; disruption of any of the yeast MCP subunits (with the exception of Y13) is lethal (Heinemeyer et al., 1994).

It has long been recognized from immunohistochemical studies that MCP subunits are found in both the cytoplasm and the nucleus (Tanaka et al., 1989), and a few of the individual subunits contain putative NLS (Tanaka et al., 1990b). We therefore undertook a series of investigations to determine which of the MCP α subunits was found in the nucleus and, more specifically, in NS. We determined that the α subunit RRC3 was found in the NS, and we then examined aspects of its regulation and potential importance in cell growth.

MATERIALS AND METHODS

These studies utilized NR4 cells, which are an SV40 immortalized, *ras* transformed rat hepatocyte cell line (Isom et al., 1992). Cells were maintained in chemically defined medium (CDM) as described previously (Woodworth et al., 1986). For some preliminary experiments, RNA was obtained from liver from male, Sprague-Dawley rats.

RT/PCR Amplification of Expressed MCP Subunits. Reverse transcription (RT)/polymerase chain reaction (PCR) amplifications were designed to amplify expressed MCP subunits and potentially to identify unknown subunits. They were conducted with 1 μg of poly(A^+) RNA, isolated from male Sprague-Dawley rat livers or the hepatocyte-derived cell line NR4. Redundant oligonucleotides were targeted to conserved regions of the α and β MCP subunits [see, for instance, Bey et al. (1993) and Tamura et al. (1992)]. For amplification of α subunits,[2] first-strand synthesis (reverse transcription) utilized the 3′ primer 3′-CWGGNAARCCV-CARWSA-5′ which was targeted to a conserved amino acid sequence motif near position 140 (Bey et al., 1993). The 5′ primer 5′-CARRTBGAATATGCHWTGRMRGCYRT-3′ was targeted to a conserved amino acid region near position 30. Additional primer pairs were also employed to amplify the specific α subunits Iota, RRC3, and RRC9. The 3′ (first-strand) primer 3′-TCCGGTGAACCAACAACA-5′ (also targeted to the region near position 140) was utilized to amplify the α subunit Iota. The 5′ primer 5′-CARRTB-GAATATGCHWTGRMRGCYRT-3′ was targeted to a conserved amino acid region near position 30. To specifically amplify α subunit RRC9, the 3′ primer 3′-GCAGGGAAAC-CACAAAGAAAC-5′ and 5′ primer 5′-CAAGTGGAATAT-GCCATGGAA-3′ were utilized. To specifically amplify RRC3, the 5′ primer was 5′-CAGATTGAATATGCTTTG-GCC-3′, and the 3′ primer was 3′-CAAGCAGGTAAAC-CACAAAGA-5′.

β subunits were amplified as three separate subfamilies. 3′ primers were targeted to amino acid sequences near position 165 (βIII subfamily) or 210 (βI and βII subfamilies), and 5′ primers were targeted to amino acid sequences near position 70. The redundant primer pairs 3′-TADATRC-CNATRCANCT-5′and5′-ATGGCNGTNSARTTYGAYGG-3′, 3′-ATRCGNATRCCNCANTACCT-5′ and 5′-TTYAART-TYCARCAYGGNGT-3′, or 3′-AARAARGGNATRATR-CA-5′ and 5′-ATHGCNGGNGARGAYTT-3′ were initially used to amplify subfamilies βI (rRing 12 and rDelta), βII (RRC1), and βIII (RRC5), respectively. However, initial attempts to amplify RRC1 was redundant primers were unsuccessful, so additional amplifications were performed with specific primers: the 3′ primer for RRC1 was 3′-ATACGGATGCCCCACTACCTG-5′, and the 5′ primer was 5′-CKTCAAATTCCAGCATGGAGTC-3′.[2]

A reverse transcription kit (Pharmacia; Piscataway, NJ) and standard conditions were used in conjunction with the

[2] W is A and T; R is A and G; S is G and C; M is A and C; Y is C and T; V is A, C, and G; B is G, T, and C; H is A, C, and T; D is A, G, and T; and N is A, T, G, and C. These are standard IUPAC–IUB nomenclature (Cornish-Bowden, 1985).

appropriate downstream α or β oligonucleotide for RT at 37 °C for 1 h. PCR reactions (50 μL) with 40 pmol of each primer were then carried out using the second upstream oligonucleotide and Taq polymerase (Perkin-Elmer; Norwalk, CT). Annealing conditions were based on the average T_m of the oligonucleotide primer pairs (which ranged from 40 to 48 °C), and were generally chosen at 3 °C below the T_m. Reactions were run for 25 cycles.

PCR products were ligated (overnight at 12 °C) into pCR II vectors and introduced into competent *Escherichia coli* cells (INVαF′) using the TA Cloning System (Invitrogen; San Diego, CA). Transformed cells from representative white colonies were grown overnight at 37 °C and subsequently used for plasmid purification with a Magic Miniprep DNA Purification System (Promega; Madison, WI). Plasmid DNAs were then sequenced utilizing standard dideoxy methods (Sequenase kits were from United States Biochemical; Cleveland, OH) in conjunction with universal M13 20-mer primers and [α-^{33}P]dATP (Amersham; Arlington Heights, IL). Sequencing was followed by standard gel electrophoresis and autoradiography.

For quantitative analyses of RRC3 and RRC9, the aforementioned specific primers and a competitive procedure were utilized, which included concurrent amplification of a 258 bp fragment (nt 581−838) from 18S rRNA. The 3′ primer used for amplification was 3′-AATCTCACAAGTTTCGTCCGG-5′, and the 5′ primer was 5′-CTTTAACGAGGATCCATTGGA-3′. Preliminary experiments varying number of cycles and amount of RNA were used to define appropriate conditions; 20 cycles with 1 μg of total RNA was found to be optimal, and 1 μCi of [^{32}P]dCTP was used per reaction. Amplifications were generally performed concurrently in triplicate.

Immunodetection of RRC3. Polyclonal antiserum was raised in rabbits against a 17 amino acid peptide (CNEAGFRRLTPTEVRDY) from the C-terminal region of rat MCP subunit RRC3 (Tanaka et al., 1990a). The peptide was coupled to keyhole limpet hemocyanin using the Imject Activated Immunogen Conjugation kit (Pierce; Rockford, IL) and subsequently sent to Cocalico Biologicals (Reamston, PA) for antiserum production. Two antiserum preparations were obtained. Serum 1 was routinely utilized: it recognized 0.05 μg of peptide at a 1:10 000 dilution in dot blot analyses (lower concentrations were not tested). Affinity-purified RRC3 antibodies were obtained by running both antisera over a column of RRC3 peptide coupled to bovine serum albumin. An ImmunoPure Ag/Ab Immobilization kit (Pierce) was used for column preparation. Affinity-purified antibodies were obtained from both antisera and gave similar results. As an additional control for immunolocalization and immunoblot analyses, preimmune sera were subjected to the same procedure.

NS preparations were isolated as previously described (Clawson et al., 1992; Tokes & Clawson, 1989), while cytosol was subsequently prepared as the 100000*g* supernate of cell homogenates. NS and cytosol proteins were separated by SDS−PAGE on 12% gels (Laemmli, 1970). Gels were run at 40 mA for 4 h and then transferred to Immobilon P (0.45 μm PVDF, Millipore; Bedford, MA) membranes using a Biorad Transblot electrophoretic transfer cell. Proteins were transferred in Tris−glycine buffer (25 mM Tris, 0.19 M glycine, 20% methanol, and 0.1% SDS) overnight at 14 V, 4 °C. Membranes were blocked (100 mM Tris, 0.1% Tween, 0.9% NaCl, and 1% dry Carnation milk) for 1.5 h before incubation with RRC3 antiserum (1:5000, 1 h). Three 10 min blocking buffer washes were done before addition of a 1:1000 dilution of the secondary, swine anti-rabbit/alkaline phosphatase antibody (Dako; Carpinteria, CA). Membranes were washed 2× in blocking buffer and 1× in TBS (100 mM Tris, pH 7.5, 0.9% NaCl) before activating the alkaline phosphatase in Genius buffer 3 (100 mM Tris, 100 mM NaCl, and 50 mM $MgCl_2$) at pH 9.5. Lumi-phos 530 (Boehringer mannheim; Indianapolis, IN) was added as a substrate before exposing the membrane to X-ray film. Typical exposures ranged from seconds to minutes. Where appropriate, quantitation of RRC3 was determined using Quantity One software (Protein Database, Inc.; Huntington Station, NY). For loading documentation, immunoblots were stripped in 60% formamide, 5 mM Tris-HCl (pH 8.0), and 1% SDS for 1 h at 75 °C, and lamin B immunodetection was done as above. However, primary antibody was mouse anti-human lamin B(Ab-1) (Oncogene Science; Uniondale, NY), and secondary antibody was swine anti-mouse/alkaline phosphatase (Dako).

Immunoprecipitations/Phosphotyrosine Identification. NS or cytosol was immunoprecipitated using protein A−Sepharose beads (Sigma) and RRC3 polyclonal antiserum, or affinity-purified antibodies. Protein A−Sepharose was preswollen in TENN (50 mM Tris, pH 7.4, 5 mM EDTA, 0.15 M NaCl, and 0.5% NP40), and 10 μL of a 50% stock was used to precipitate RRC3 from 1000 μg of NS protein. Precipitations were performed in 1 mL of TKMC (50 mM Tris, pH 7.4, 25 mM KCl, 5 mM $MgCl_2$, and 10 μM $CaCl_2$) containing a protease inhibitor cocktail (Tokes & Clawson, 1989) and were conducted overnight at 4 °C. Following precipitation, the protein A−Sepharose beads were collected and washed 3× in SNNTE (0.15 M sucrose, 0.5 M NaCl, 1% NP40, 50 mM Tris, pH 7.4, and 5 mM EDTA), and 1× in RIPA (50 mM Tris, pH 7.4, 0.15 M NaCl, 1% Triton X-100, 0.1% SDS, and 24 mM deoxycholic acid). Beads were then boiled in SDS sample buffer, and gel electrophoresis and immunodetection were performed as previously stated. However, the primary antibody was $IgG2b_k$, a mouse monoclonal antibody directed against phosphotyrosine (Upstate Biotechnology Incorporated; Lake Placid, NY), and the secondary antibody was goat anti-mouse/alkaline phosphatase (Dako).

For metabolic [^{32}P]orthophosphate labeling studies, four 100 mm plates of NR4 cells (10^7 cells/plate) were each incubated with 300 μCi of [^{32}P]orthophosphate (Amersham, specific activity 9000 Ci/mmol) in CDM. After 24 h, cells were harvested by scraping and rinsed, and NS and cytosol were prepared as described. For comparative purposes, in some experiments cells were lysed and a crude pellet was obtained by centrifugation at 2000*g* for 5 min at 4 °C. This pellet was then rinsed with TKMC containing 1% Triton X-100, and nuclei were isolated by centrifugation through a 1 M sucrose−TKMC cushion at 16000*g* for 5 min at 4 °C.

Proteasome Purification. Purified rat liver nuclei were lysed by sonication for 1 min at 0 °C in TKMCD (TKMC containing 1 mM DTT, dithiothreitol). Sonicated nuclei were then centrifuged for 30 min at 20000*g*, and the supernate was loaded onto a Q-Sepharose (Pharmacia Biotech; Piscataway, NJ) chromatographic column. Bound material was eluted with a salt step gradient of 0.1, 0.3, 0.4, and 1.0 M NaCl, and the eluate was monitored for proteolytic activity. Activity was measured with the synthetic peptide substrate

$LLVY_{AMC}$ (LLVY-7-amino-4-methylcoumarin, Enzyme Systems Products; Livermore, CA) as described below. However, reactions contained 25 μM substrate in a final volume of 100 μL. Proteolytically active fractions were concentrated and applied to an HPLC Protein-Pak 300SW column (Waters; Milford, MA) for further purification of proteasomes. Proteasomes from cytosol (20000*g* supernatant of rat liver homogenates) were also purified by HPLC followed by Q-Sepharose chromatography as described.

In Situ Localizations. *In situ* localizations utilized NR4 cells. For these experiments, NR4 cells were grown on Probeon glass slides (Fisher; Pittsburgh, PA) for 1 day. The slides were then washed with PBS (0.14 M NaCl, 2.7 mM KCl, 10 mM Na_2HPO_4, and 1.8 mM KH_2PO_4), and fixed in PBS containing 4% paraformaldehyde for 15 min. They were then washed with PBS, and incubated for 5 min in 0.2 N HCl (to inhibit endogenous alkaline phosphatase), followed by washing in PBS to restore pH. Blocking was for 20 min with PBS containing 5% normal goat serum (Vector; Burlingame, CA), 10% fetal bovine serum (Gibco; Gaithersburg, MD), and 0.3% Triton X-100. Incubation with the primary antibody, rabbit anti-RRC3, was done with affinity-purified antibodies at equivalent 1:200 dilutions in PBS containing 1% normal goat serum and 0.3% Triton X-100 overnight at 4 °C. Cells were then rinsed in PBS, and incubated in a 1:300 dilution of secondary antibody, which was a biotinylated goat anti-rabbit antibody (Vector). After 1 h, cells were again washed with PBS and then incubated for 1 h with a 1:200 dilution of Vectastain ABC reagent (Vector) in PBS containing 0.3% Triton X-100, 0.2 M methyl pyranoside, and 0.3 M NaCl. Cells were then washed in PBS before activation of alkaline phosphatase in 100 mM Tris-HCl (pH 9.5) containing 0.1 M NaCl and 0.05 M $MgCl_2$. BCIP and NBT chromagen were then added at twice the manufacturer's recommended concentrations for 10 min at room temperature in the dark. The reaction was stopped with 10 mM Tris-HCl (pH 7.5) containing 1 mM EDTA and 0.15 M NaCl. Coverslips were mounted using Glycergel mounting medium (Dako), and slides were examined using an Olympus BH-2 microscope, planApo lenses, and an Olympus autoexposure photography setup.

Antisense Oligonucleotide Studies. Antisense/sense phosphorothioate oligonucleotides (s-oligonucleotides) were obtained from National Biosciences (Plymouth, MN). Both antisense (5′-GCTGTAACCGCGTTCTGCCAT-3′) and sense (5′-ATGGTTGAGGACGATGCCTGC-3′) phosphorothioate oligonucleotides were targeted to the initiation site of rat RRC3. The sense oligonucleotide was designed with 50% mismatches incorporated, but with identical AT/GC content.

For standard experiments, NR4 cells were plated at a density of 1×10^5 cells/60 mm dish in CDM containing 3% FCS. The medium was changed to CDM at 4 h, and the cells were maintained as before; medium was changed every other day. Time and dose curves were generated by transfecting NR4 cells for different periods of time and with various amounts of antisense/sense phosphorothioate oligonucleotides, using Lipofectin (Gibco) as an oligonucleotide carrier. Incubations with the Lipofectin/phosphorothioated oligonucleotides were for 2, 4, or 6 h at 37 °C. Lipofectin (40 μL) with 0.1, 0.2, 0.5, or 1.0 μM oligonucleotide (final concentration) was added to a total volume of 4 mL of OPTI-MEM I media (Gibco). After the appropriate incubation time, the medium was changed to CDM, and cells were generally maintained for 4 days before being trypsinized and counted. Triplicate assays were performed, and data were analyzed using a Student's *t*-test.

Stability of the phosphorothioate oligonucleotides was determined by transfecting cells with ^{32}P end-labeled oligonucleotide. Oligonucleotides were end-labeled with [γ-^{32}P]-ATP (NEN; Boston, MA) and T4 polynucleotide kinase (Promega) for 1.5 h at 37 °C. Cells were then transfected with Lipofectin/0.2 μM oligonucleotide for 4 h (as above) and collected 2 and 4 days later. Cells were rinsed, and total cell volume was measured. Cells were then lysed with 1% Triton X-100, and extracted twice with phenol/chloroform before precipitable counts were collected and counted on Whatman GF/C filters. Parallel controls (end-labeled oligonucleotide alone, and labeled oligonucleotide added to cells just prior to lysis) were run to assess recoveries.

Effects of Lipofectin/Oligonucleotide Treatment on RRC3 Protein, RRC3 mRNA, and NS Protease Activity. For these experiments, 20 plates of NR4 cells were seeded (7.5×10^5 cells/100 mm dish) and grown for 24 h. Cells were then treated with Lipofectin only, Lipofectin/sense RRC3 oligonucleotide, or Lipofectin/antisense RRC3 oligonucleotide under our standard conditions (0.2 μM oligonucleotide with Lipofectin for 4 h at 37 °C). Following treatment, cell plates were washed, and fresh CDM was added. Medium was changed 2 days later, and cells were harvested after 4 days (day 5) by scraping. Cells were disrupted by homogenization in TKMC buffer containing 1% Triton X-100, and a crude nuclear pellet was collected by centrifugation at 2000*g* for 5 min at 4 °C. The pellet was resuspended in 0.25 M $STKM_2$ (sucrose of the specified molarity, 50 mM Tris, pH 7.4, 25 mM KCl, 5 mM $MgCl_2$, and 5 mM 2-mercaptoethanol), and nuclei were purified as described (Clawson et al., 1992). Cytosol was obtianed as the 100000*g* supernate, after homogenization in the absence of detergent. NS was prepared from purified nuclei, and protein concentration was determined by the method of Lowry (Lowry et al., 1951). RRC3 was detected by the immunoblot procedure described.

Northern blot analyses were conducted as described (Ausubel et al., 1994) using 5 μg total RNA with formaldehyde gels and a Magnagraph nylon membrane (Micron Separations, Inc.; Westborough, MA). RNA was cross-linked using UV irradiation (Stratalinker from Stratagene; La Jolla, CA). The filter was then prehybridized in buffer containing 50% formamide (Ausubel et al., 1994), and hybridization was for 24 h at 42 °C with $(1-5) \times 10^6$ cpm/mL of ^{32}P-labeled probe. Probes were RRC3 or 18S RT/PCR products (see above), which were labeled by random priming (Prime-a-Gene kits from Promega). Posthybridization rinses were as described (Ausubel et al., 1994), with final washes at 42 °C (RRC3) or 55 °C (18S) in 0.1× SSC. Membranes were then exposed to film for autoradiography at −70 °C with intensifying screens.

For characterization of NS protease activity, NS preparations were employed with a number of protease assays. Our standard assay utilized the thiobenzyl ester $_{ms}AAPF_{sb}$ (methoxysuccinyl-AAPF-*S*-benzyl). Twenty micrograms of NS preparations (from either RRC3 antisense treated, sense treated, or untreated preparations) was incubated with 1 mM $_{ms}AAPF_{sb}$, in a final volume of 1 mL of TKMC containing 10% dimethyl sulfoxide, for 5 h at 37 °C as previously described (Clawson et al., 1992). After incubation, A_{324} absorbances were read; blanks (no NS, and boiled NS) were

run as controls. For additional proteolytic assessments, the fluorescent trypsin substrate R_{AMC} and the chymotrypsin substrate $LLVY_{AMC}$ (Enzyme Systems Products) were utilized. Reactions containing 5 μg of NS protein were run with 1 mM substrate in 50 μL capillary tubes, and fluorescence was monitored in a Hoefer (San Francisco, CA) DNA fluorometer (excitation was at 365 nm, and emission was monitored at 460 nm). Additional reactions for proteolytic activity utilized denatured ^{3}H-collagen (Amersham, specific activity 0.19 mCi/mg); assays contained 10 μCi of labeled substrate and 10 μg of NS protein, and were conducted for 3 and 6 h at 37 °C. Proteolytic activity was assessed by measuring soluble ^{3}H after precipitation with 10% trichloroacetic acid, and linear regression slopes were obtained from the time-course data.

Flow Cytometry. NR4 cells were transfected with Lipofectin/0.2 μM antisense or sense oligonucleotide for 4 h as described. Approximately (1−2) × 10^6 cells were collected after 4 day (or 6 day) treatments and resuspended in cryopreservation media (0.3 M NaCl, 15% DMSO, and 20% FCS in CDM). Cells were then stained for DNA content in the dark with 1 mL of fluorochrome buffer (0.1 sodium citrate, pH 7.4, 20 μg/mL RNase A, 0.3% NP40, and 50 μg/mL propidium iodide) for 1 h. Cells were then passed through a 27$^1/_2$ gauge syringe and analyzed on a Coulter Epics V flow cytometer using a Coherent Inova 90-5 laser at 400 mW and 488 nm. Data were analyzed with a Multiparameter Data Acquisition and Display System. Analyses were done at the core Flow Cytometry Facility at Penn State University.

RESULTS

Initial RT/PCR experiments were conducted with redundant primers to highly conserved regions, both to determine whether additional unknown subunits could be identified as well as to determine the repertoire of MCP subunits expressed in rat hepatocytes. No unknown MCP subunits were identified, while nine known MCP subunits were amplified. Of these expressed subunits, the α subunit RRC3 was most frequently encountered, representing nearly 80% of the MCP transcripts amplified with the redundant primers. RRC3 was of particular interest because it contains a putative NLS [EKKQKSIL (Tanaka et al., 1990b)] analogous to that of SV40 T-antigen and lamins. Other expressed α subunits obtained using the redundant primers were RRC8, RRC2, and Iota, and the sequences obtained matched those reported in the databases. Initial attempts to amplify RRC9, the other rat MCP α subunit with a putative NLS, were unsuccessful. However, we subsequently obtained RRC9 using specific primers, although it was present at much lower levels than RRC3 as demonstrated on Northern blots (and by quantitative competitive RT/PCR).

Similar RT/PCR amplifications of β subunit subfamilies yield rDelta, RRC5, and rRing 12, but initial attempts to amplify RRC1 with redundant primers were not successful (RRC1 is the rat homolog of human Ring 10, a β subunit which may participate in chymotrypsin-like peptidase activity). However, RRC1 was obtained using specific primers. With regard to rRing 12, multiple clones contained a base change at position 377 (from A to G) which results in an amino acid change of H to R. While the published rRing 12 sequence contains an H at this position (Tamura et al., 1992), an R is is present at the equivalent position in the human MCP subunit (Ring 12). In rRing 12, additional third position changes were also found at nucleotides 366 (T to G), 435 (G to A), and 441 (C to T) although these would not entail amino acid changes. It therefore appears that the full repertoire of MCP subunits is expressed in hepatocytes, and that RRC3 represents a highly expressed subunit.

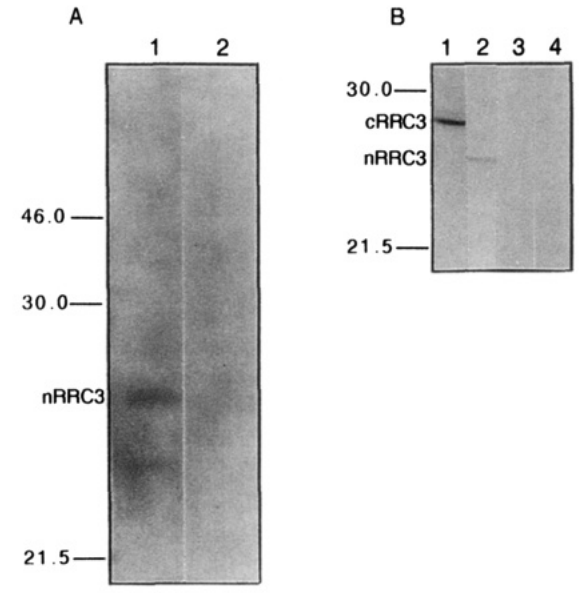

FIGURE 1: Nuclear scaffold localization of rat MCP α subunit RRC3. (A) NS proteins were separated by SDS−PAGE and transferred to Immobilon P Membranes. RRC3 was observed in the NS preparations with anti-RRC3 antiserum (lane 1), but was not observed with preimmune serum (lane 2). Nuclear RRC3 was observed as a single band of M_r 24 000. (B) RRC3 antiserum was used for immunodetection of RRC3 in cytosol (cRRC3) or NS (nRRC3). Immunodetected RRC3 protein showed a M_r of 28 000 in cytosol (lane 1) vs 24 000 in NS (lane 2). Bands were not observed when equivalent amounts of cytosol (lane 3) or NS (lane 4) were stained with preimmune serum.

On the premise that RRC3 may represent a nuclear α subunit, which might also possibly function in coupled nuclear translocation of an as yet undefined β catalytic subunit, we undertook further studies on RRC3. RRC3 antiserum was developed by immunization of rabbits with the peptide CNEAGFRRLTPTEVRDY, from the C-terminal portion of RRC3. This region is unique to RRC3, differing considerably from sequences found in other MCP α subunis, and was predicted to be highly antigenic based on computer analysis. RRC3 affinity-purified antibodies were subsequently used in immunoblot analyses, immunoprecipitations, and *in situ* localizations. Immunoblot analyses demonstrated the presence of RRC3 in both cytosol and NS preparations from NR4 cells (Figure 1). Quantitatively, most RRC3 was present in the cytosol. Qualitatively, however, there was a clear difference; cytosolic (M_r 28 000) and NS (M_r 24 000) forms differed considerably in their M_rs (Figure 1B, lanes 1 and 2), with the nuclear form (nRRC3) migrating significantly faster. Both the NS and cytosolic forms were recognized by affinity-purified antibodies from both antisera.

Since phosphorylation of RRC3 on a tyrosine residue (amino acid 121) has been speculated to be a potential modification, NS and cytosolic proteins were immunoprecipitated with RRC3 antibodies, separated by PAGE, and electrophoretically transferred to filters, which were then detected with anti-phosphotyrosine antibodies. The results showed that the NS form of RRC3 contains phosphotyrosine

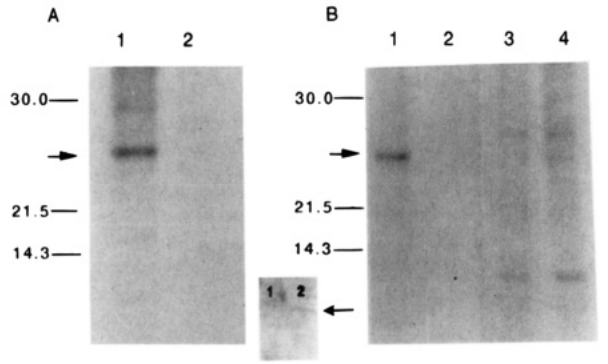

FIGURE 2: Differential phosphorylation of NS vs cytosolic RRC3. (A) Nuclear and cytosolic proteins were labeled by incubation of NR4 cells with [^{32}P]orthophosphate. Nuclear and cytosolic fractions were then prepared and were immunoprecipitated with affinity-purified anti-RRC3 antibodies, and then separated by SDS−PAGE. A major phosphorylated band was seen at M_r 24 000 in the nuclear fraction, as was a minor band of M_r 28 000 (lane 1). Neither of these bands was detectable in cytosolic proteins (lane 2). (B) NS and cytosolic fractions were prepared from NR4 cells after metabolic labeling with [^{32}P]orthophosphate. NS and cytosolic proteins were immunoprecipitated with affinity-purified anti-RRC3 antibodies and separated by SDS−PAGE. Again, the M_r 24 000 band was observed in NS (lane 1), but not in cytosol (lane 3). The M_r 28 000 band was not present in NS. Controls were also run without primary antibody (NS, lane 2; cytosol, lane 4). The inset shows an RRC3 immunoprecipitate similarly prepared and detected with antibodies against phosphotyrosine: nuclear scaffold RRC3 contains phosphotyrosine (lane 2), whereas the cytosolic form (lane 1) does not.

while the cytosolic form of RRC3 does not (Figure 2, inset). Since this procedure approached detection limits, additional experiments were subsequently performed after labeling NR4 cells *in vivo* with [^{32}P]orthophosphate. Immunoprecipitations with affinity-purified RRC3 antibodies, followed by SDS−PAGE and autoradiography, showed no labeling of M_r 28 000 cytosolic RRC3 (Figure 2A, lane 2). However, the major M_r 24 000 NS form was labeled with ^{32}P (Figure 2B, lane 1). To address the possibility that the apparent reduction in M_r of immunoreactive NS RRC3 was an artifact of the NS preparation procedure, we also utilized rapidly isolated nuclei in immunoprecipitations after [^{32}P]orthophosphate labeling of cells. The M_r 24 000 form observed in NS preparations was again the major form present (Figure 2A, lane 1), although a faint band at M_r 28 000 was also detected. Together, thse results clearly document differential tyrosine phosphorylation of the nuclear form of RRC3, and suggest that this modification may participate in targeting RRC3 to the nucleus (see Discussion).

In an attempt to further define the nuclear localization of RRC3, nuclei were disrupted by sonication, and separated into nucleoplasmic (soluble) and insoluble fractions, and NS was prepared from the insoluble portion. Approximately half of the total nuclear protease activity was solubilized by this procedure. The nuclear extract was then separated sequentially on ion-exchange and HPLC gel-filtration columns (Figure 3A,B). Most of the soluble nuclear protease activity was found in very large complexes (>M_r 700 000), characteristic of MCPs, with a 130−250× enrichment in specific activity. The equivalent fraction was obtained for cytosolic preparations for comparative purposes (Figure 3C). Immunoblot analyses showed that RRC3 was present in the isolated MCP complexes with M_r 28 000 (Figure 3D). The major M_r 24 000 form was not present in the soluble nuclear fraction (see Discussion). Using antiserum raised against bovine 20S MCP, we also observed strong immunostaining (Figure 3D) of another MCP component (M_r 32 000), and longer exposures disclosed weak staining of three additional MCP subunits (M_rs of 34 000, 28 000, and 26 000). We were not able to solubilize the NS MCP activity without using harsh conditions, so the question of whether NS RRC3 is present within MCP complexes could not be resolved.

Nuclear localization of RRC3 was also examined *in situ*, again using anti-RRC3 antibodies and standard alkaline phosphatase immunohistochemistry. Most of the staining observed in NR4 (and rat liver) cells was observed in the cytoplasm, as expected (Figure 4B,C), where it showed a punctate pattern. In addition, however, clear nuclear staining was also observed (Figure 4D−G). The nuclear staining was always present but was variable in appearance. In most cases, strong staining of the nuclear perimeter was evident (Figure 4F,G). This nuclear localization was identical to results obtained with $_{\text{biotin}}$AAPF$_{\text{cmk}}$ (a biotinylate, irreversible chloromethyl ketone inhibitor targeted to chymotrypsin-like activity) after digitonin/ionomycin permeabilization of NR4 cells (Clawson et al., 1995).

Experiments were subsequently undertaken using antisense and sense phosphorothioated oligonucleotides targeted to the translational start site of RRC3. Using NR4 cells, preliminary experiments were done to examine a variety of oligonucleotide treatments (including both time and dose curves) and to determine the most effective treatment conditions. A 4 h treatment (1×10^5 cells) with Lipofectin/0.2 μM antisense or sense oligonucleotide appeared optimal (Figure 5A,B); these conditions produced little or no significant growth inhibition with the sense phosphorothioated oligonucleotide compared to Lipofectin only treatment, whereas the antisense oligonucleotide produced 60% and 95% inhibition of cell growth at 0.1 μM and 0.2 μM (respectively). These conditions (0.2 μM/4 h) were therefore adopted as standard in subsequent studies. The intracellular concentration of oligonucleotide under these treatment conditions (based on total cell volumes and oligonucleotide uptake) was 17 μM after the initial treatment (Figure 5C). The stability of the oligonucleotide in NR4 cells was determined by phenol extraction and precipitation of intact, end-labeled oligonucleotide at 2 and 4 days (day 3 and day 5) after treatment (Figure 5D). At day 3, at least 44% of the oligonucleotide remained in the NR4 cells while at day 5 about 30% remained, yielding an intracellular concentration of 5 μM. Treatments of 4 days duration were therefore used in subsequent studies.

When NR4 cells were treated under our standard conditions (Lipofectin/0.2 μM oligonucleotide for 4 h), RRC3 antisense oligonucleotides produced dramatic inhibition of cell growth. A 94% reduction in cell growth (significant at $p < 0.001$) was observed upon treatment with antisense RRC3 as compared to untreated, sense-treated, or Lipofectin-treated NR4 cells (Figure 6). Cell number remained essentially constant in antisense-treated preparations, reflecting a cytostatic effect, with no evidence of overt toxicity. To determine the effects of antisense/sense oligonucleotides on RRC3 levels, RNA, NS, and cytosol were prepared from treated cells (0.2 μM/4 h) and examined. At the highest growth inhibitory levels, mRNA for RRC3 was barely detectable by Northern blot analyses in antisense-treated cells, while sense-treated cells showed a single band at 1.1 kb

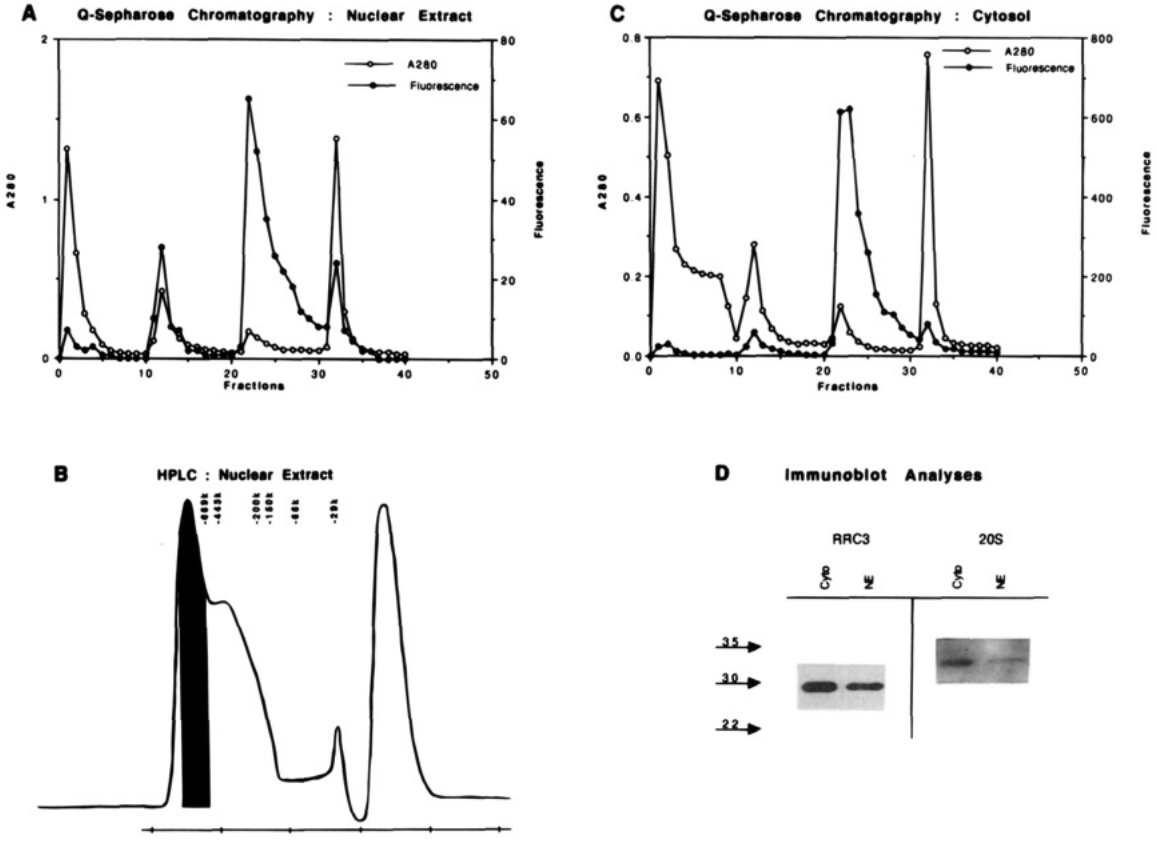

FIGURE 3: Immunodetection of RRC3 in soluble nuclear and cytosolic MCPs. (A) Soluble nuclear extract was loaded on a Q-Sepharose chromatographic column, and bound protein was eluted with 0.1, 0.3, 0.4, and 1.0 M NaCl. Proteolytic activity was monitored and found to be predominantly in the 0.4 M NaCl elute (fractions 20−27). (B) Proteolytically active nuclear extract fractions were further separated by HPLC. Proteolytic activity was concentrated in large (>700 000 M_r) MCP complexes (denoted by the shaded area of the HPLC absorbance profile). (C) Cytosolic proteins were also separated by Q-Sepharose chromatography, and proteolytic activity was again observed in the 0.4 M NaCl elute (fractions 20−27). (D) Purified MCPs from cytosol and nuclear extract were separated by SDS−PAGE and transferred to Immobilon P membranes for immunoblot analyses. Using RRC3 antibody, a single band of M_r 28 000 was observed in both cytosol (Cyto) and nuclear extract (NE) MCPs. The blot was then stripped and reprobed with an antiserum directed against 20S bovine MCP: This revealed a predominant band with M_r 32 000. Longer exposures revealed three additional bands with M_rs of 34 000, 28 000, and 26 000.

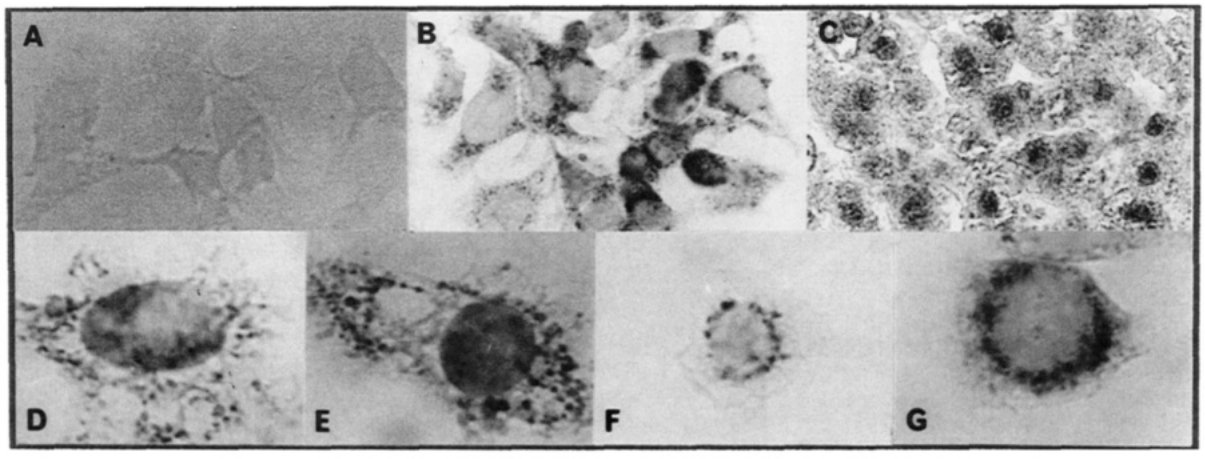

FIGURE 4: *In situ* localization of RRC3. NR4 cells were grown on glass slides for 24 h, were processed as described, and were stained with affinity-purified anti-RRC3 antibody and standard alkaline phosphatase immunohisotochemial procedures. RRC3 protein in NR4 cells (and in frozen liver sections) was predominantly localized in the cytoplasm (panels B and C, respectively). In addition, however, prominent nuclear staining was also observed in NR4 cells (D−G). In most cells, the nuclear staining was most intense at the nuclear periphery (F and G). As a negative control, NR4 cells stained with equivalent fractions from preimmune serum are shown in panel A.

(Figure 7), and the level of RRC3 mRNA quite closely reflected the extent of growth inhibition in individual experiments (not shown). This reduction is estimated to represent at least 95%. As a loading control, 18S rRNA was also assessed; although RNA loading was heavier in the sense-treated lane, the differential effects of the treatment are clear (Figure 7).

With immunoblot analyses, we observed a dramatic reduction in RRC3 protein levels in NS (Figure 8): RRC3 was not detectable in NS preparations from antisense-treated cells, indicating a reduction of greater than 80% (based on detection limits). In contrast, cytosolic RRC3 protein levels were relatively unaffected, showing a reduction of about 25% (see Discussion). The notable difference in M_r between

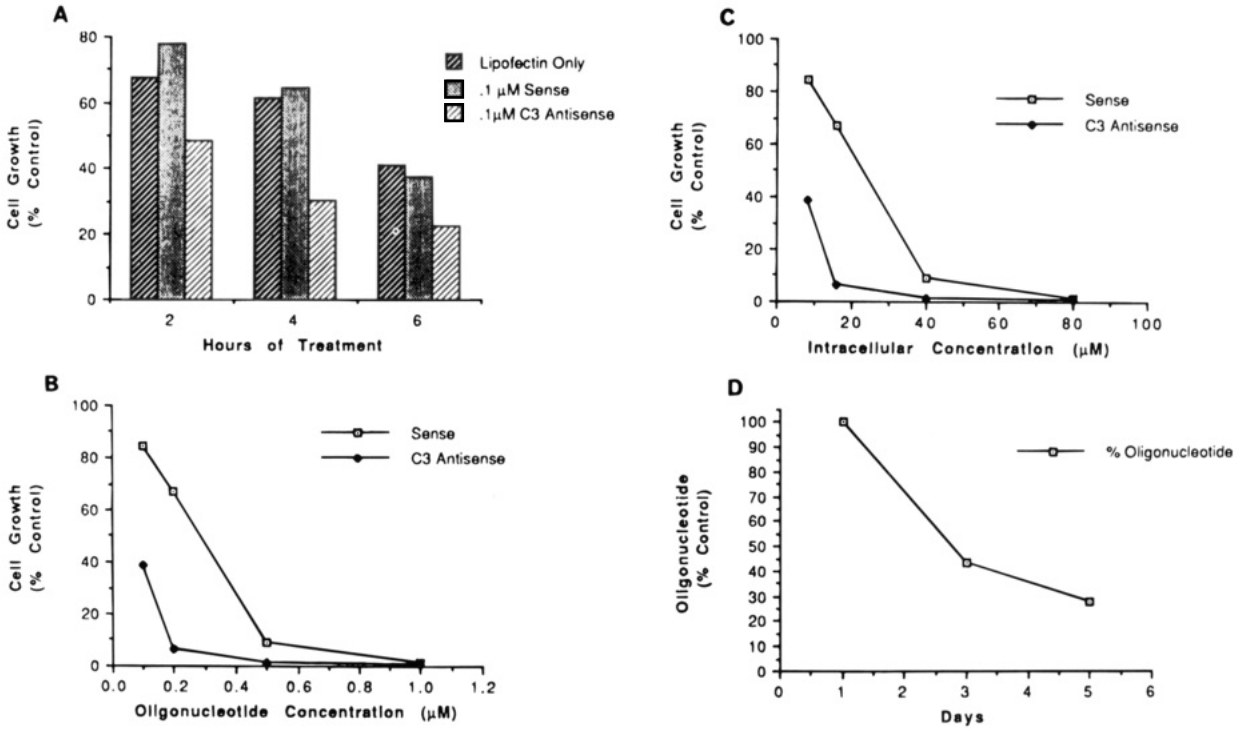

FIGURE 5: Effects of antisense oligonucleotides on NR4 cell growth. (A) NR4 cells were plated and after 24 h (day 1) were transfected with Lipofectin/0.1 μm RRC3 antisense or sense oligonucleotide or Lipofectin only, or were untreated for 2, 4, or 6 h. Cells were then washed and maintained for 4 days in CDM and then counted. Cell counts are shown as a percentage of the control cell number (untreated) at day 5, and represent means of triplicate plates. (B) NR4 cells were transfected with Lipfectin/0.1, 0.2, 0.5, or 1.0 μM RRC3 antisense or sense oligonucleotide for 4 h. Cells were maintained for 4 additional days and counted. The cells remaining after each treatment are shown as a percentage of control cells (untreated) at day 5. Percentages are the mean of triplicate plates. (C) Data from (B) are plotted as percent control vs intracellular concentrations of oligonucleotide. This concentration is based on the measured volume of each cell pellet and the uptake of ^{32}P-labeled oligonucleotide. (D) Stability of ^{32}P-labeled phosphorothioated oligonucleotides. Oligonucleotides were end-labeled with T4 kinase, and used in Lipofectin/0.2 μM transfections. After 2 or 4 days (day 3 and day 5), cells were harvested and lysed, and DNA was extracted, precipitated, and counted. Controls included aliquots to which labeled oligonucleotide was added just prior to cell lysis. Values shown are means of triplicate determinations. Individual replicate determinations varied by approximately 10%. Antisense oligonucleotide-treated cell counts differed significantly from sense-treated or control cells counts for 2 and 4 h Lipofectin treatments at $p < 0.001$ by the Student's t-test.

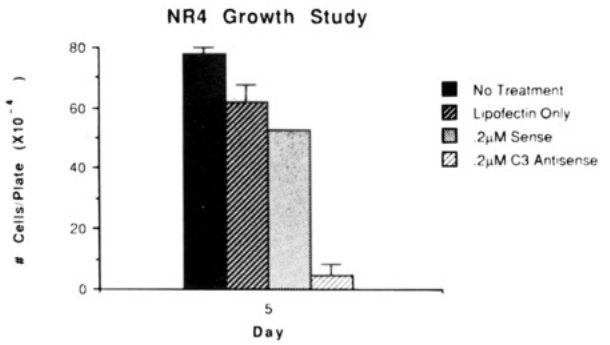

FIGURE 6: Effects of standard RRC3 antisense oligonucleotide conditions on growth of NR4 cells. NR4 cells were plated (at 1×10^5/60 mm dish) and 24 h later (designated as day 1) either were transfected with Lipofectin/0.2 μM RRC3 antisense or sense oligonucleotide or Lipofectin only or were untreated. After 4 h, cells were rinsed and maintained for 4 days in CDM, after which cell counts were obtained. Values represent means $\pm$ standard deviations from triplicate plates. The antisense-treated cells counts differed at $p < 0.001$ from untreated or sense-treated counts.

nuclear and cytosolic forms of RRC3 was again evident (Figure 8). Lamin B antibodies were then used for immunodetection to confirm equal loading of sense and antisense proteins (Figure 8, bottom). Similar loading controls for cytosol preparations were performed with S6 kinase (data not shown).

When chymotrypsin-like NS peptidase activity was assessed, no significant difference in activity of the NS protease from RRC3 antisense vs sense oligonucleotide-treated cells was observed. Using $_{ms}AAPF_{sb}$ substrate, the NS peptidase activity of RRC3 antisense vs sense oligonucleotide-treated cells was 3.5 $\pm$ 0.4 and 3.4 $\pm$ 0.1 A_{324} units/(h·mg) (respectively), compared with 3.1 A_{324} units/(h·mg) for untreated cells (see Discussion). Similar results were obtained with the fluorescent chymotrypsin substrate $LLVY_{AMC}$. When trypsin-like peptidase activity was assessed with R_{AMC} in NS preparations from antisense- vs sense-treated or control cells, no activity was observed for any of the preparations. This is in contrast to our previous results with thiobenzyl ester substrate, where we found a small amount of trypsin-like activity (Clawson et al., 1992). General protease activity was then determined using denatured ^{3}H-collagen as a substrate. Again, no change in the rate of degradation was observed in NS preparations from antisense-treated vs control-treated cells (1750 and 1450 ^{3}H-solubilized cpm/h, respectively). HPLC analyses (as described) indicated no change in the amount of MCP present in the soluble nuclear compartment following antisense oligonucleotide treatment, and there was also no change in total nuclear proteolytic activity (data not shown).

We also considered the possibility that RRC9, the other α subunit with a putative NLS, might have been up-regulated to compensate for dramatic reductions in RRC3 levels. However, quantitative competitive RT/PCR and Northern analyses showed that there was no compensatory increase

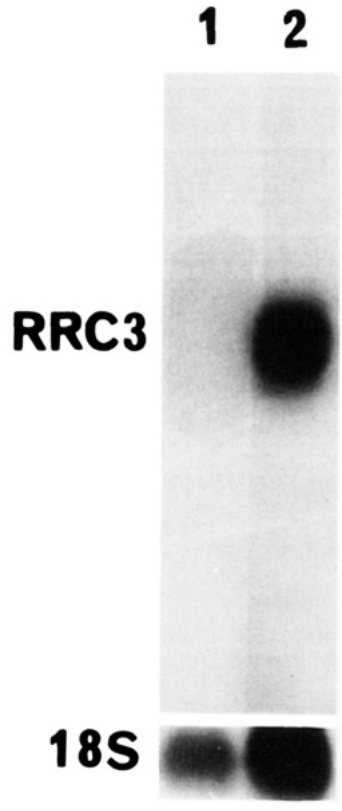

FIGURE 7: Northern blot analysis of RRC3. RNA from NR4 cells treated with sense or antisense oligonucleotides was purified and used in Northern blot analysis. RRC3 was detected as a single 1.1 kb band in sense-treated RNA (lane 2), but was barely detectable in RNA from antisense oligonucleotide-treated cells (lane 1). The blot was then stripped and rehybridized with an 18S rRNA probe to document RNA loading. In this case, roughly twice as much sense RNA was present, although the marked reduction in RRC3 mRNA was still obvious.

in RRC9 levels following antisense treatment (data not shown).

To determine if the cell growth inhibition observed was a result of a specific cell cycle block, NR4 cells were treated for 4 h with Lipofectin/0.2 μM antisense or sense oligonucleotide and collected 4 days later. The cells were then stained for DNA content and examined by flow cytometry (Figure 9). RRC3 antisense-treated cells showed no change in DNA profile from sense-treated or untreated cells after 4 day treatments, and similar results were obtained after 6 day treatments. These results demonstrate that the growth inhibition is not associated with any block at a specific stage of the cell cycle.

In concert with inhibition of cell growth, a dramatic morphological change was observed in NR4 cells upon treatment with RRC3 antisense oligonucleotide (Figure 10). Cells transfected with RRC3 antisense oligonucleotide showed no evidence of overt toxicity; they had a more round, compact structure, and were found in tightly packed islands on otherwise sparsely populated plates (Figure 10). This morphology is reminiscent of CWSV16 cells, an SV40-immortalized cell line (derived in parallel to the parental CWSV1 cell line), which have a relatively organized actin cytoskeleton with both thick and fine filaments (Isom & Hu, 1993). Both RRC3 antisense-treated and untreated cells were therefore stained with phalloidin/rhodamine to observe actin cytoskeletal organization. RRC3 antisense-treated cells, however, retained the unorganized cytoskeletal actin pattern typical of NR4 cells (data not shown).

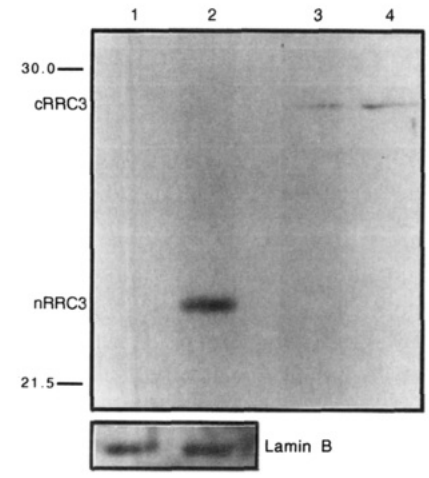

FIGURE 8: Effects of RRC3 antisense oligonucleotide on RRC3 protein levels in NR4 cells. NR4 cells were transfected with Lipofectin/0.2 μM antisense or sense oligonucleotide, and after 4 h, the cells were rinsed and subsequently maintained in CDM for 4 days. At day 5, cells were harvested, and NS and cytosol were collected. Immunodetection of RRC3 in NS and cytosolic fractions showed a complete loss of RRC3 from NS from antisense vs sense oligonucleotide-treated NR4 cells (lanes 1 and 2, respectively), but only a small reduction in cytosolic RRC3 from antisense vs sense-treated cells (lanes 3 and 4, respectively). The blot was then stripped, and lamin B detection (lanes 1 and 2, bottom) demonstrated equal loading of NS proteins. Equal loading of cytosolic proteins was checked using S6 kinase (data not shown).

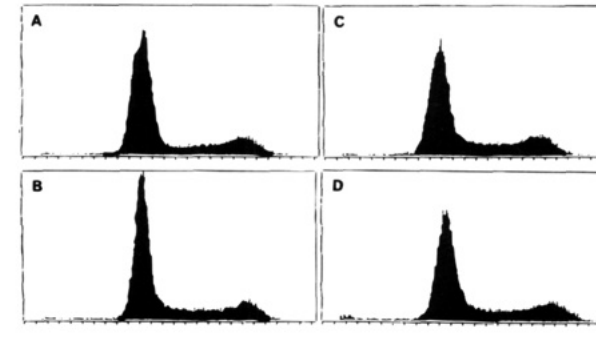

FIGURE 9: DNA content analysis of NR4 cells treated with RRC3 antisense oligonucleotides. NR4 cells either were transfected with Lipofectin/0.2 μM RRC3 antisense or sense oligonucleotide or Lipofectin only or were untreated. After 4 h, they were rinsed and maintained in CDM for 4 days. The cells were then harvested, stained for DNA content with propidium iodide, and examined by flow cytometry. Figures show representative analyses of NR4 cells after: (A) no treatment; (B) Lipofectin only; (C) RRC3 sense oligonucleotide treatment; and (D) RRC3 antisense oligonucleotide treatment. Similar results were obtained 6 days after treatment.

DISCUSSION

In this study, we demonstrated that the MCP α subunit RRC3 is present in the nucleus and cytoplasm. However, nuclear RRC3 differs substantially from its cytoplasmic counterpart, and a number of aspects of our results merit discussion. First, nuclear and cytoplasmic RRC3 forms differ significantly in M_r. Second, the nuclear forms also contain phosphotyrosine, whereas the cytoplasmic form does not. Third, antisense oligonucleotide treatment differentially affects the nuclear form, while producing profound effects on cell growth and morphology.

Of particular interest was the finding that the NS form of RRC3 migrated significantly faster than the cytosolic form,

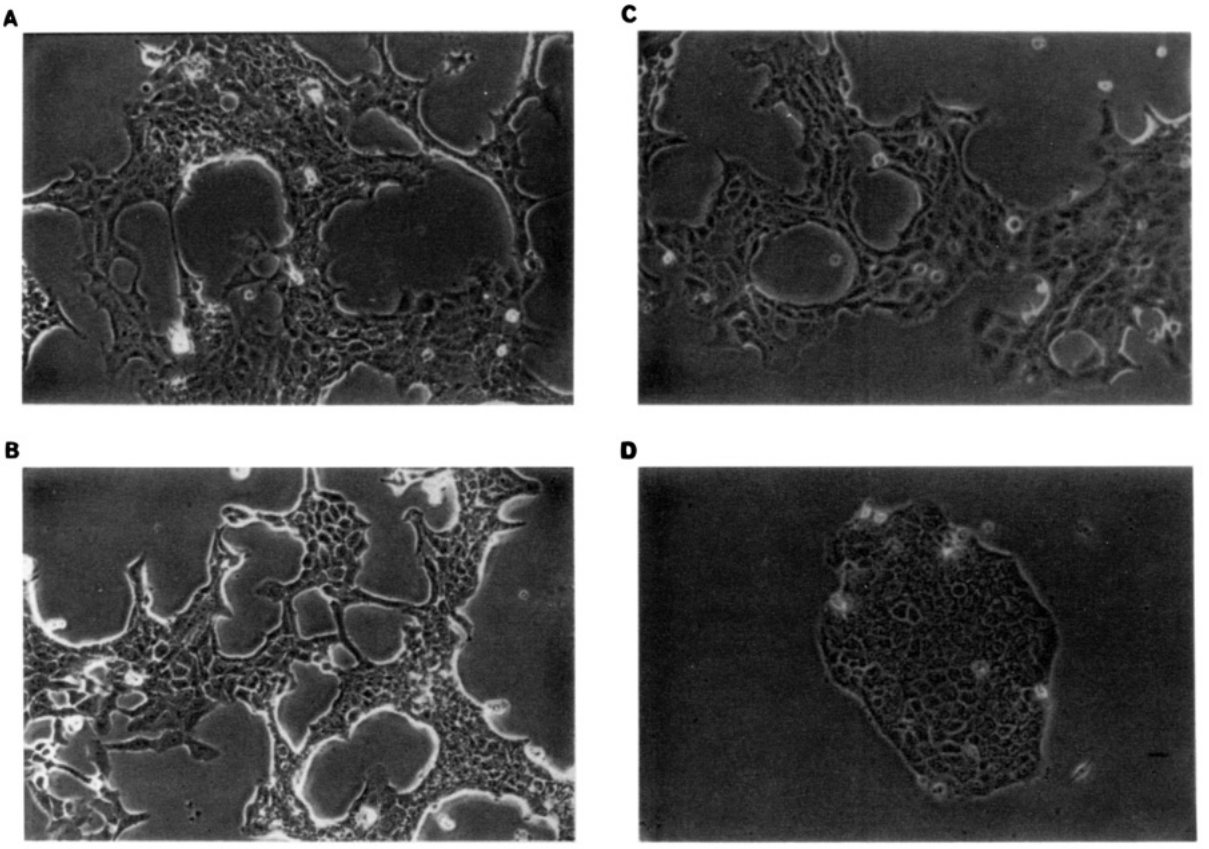

FIGURE 10: Effects of RRC3 antisense oligonucleotides on the morphology of NR4 cells. NR4 cells either were transfected with Lipofectin/0.2 μM RRC3 antisense or sense oligonucleotide or Lipofectin only or were untreated for 4 h. Cells were then rinsed and maintained for 4 days in CDM, after which they were photographed with a phase contrast microscope. Representative photomicrographs show NR4 cells after: (A) no treatment; (B) Lipofectin only; (C) RRC3 sense oligonucleotide treatment; and (D) RRC3 antisense oligonucleotide treatment. Cells treated with RRC3 antisense oligonucleotides show a distinct morphological change, from that typical of NR4 cells to a more rounded, smaller, and more compact aggregate. The bar represents approximately 40 μM.

with an apparent M_r of 24 000 vs 28 000 for the cytosolic form. Since the antibody used for detection is directed against the C-terminal portion of RRC3, the most likely explanation for this result is that the NS RRC3 is truncated N-terminally (see below). Indeed, some processing of MCP subunits has been noted previously (Kreutzer-Schmid & Schmid, 1990; Weitman & Etlinger, 1992; Fruh et al., 1994; Frentzel et al., 1994; Seeling et al., 1993). For example, the β subunits LMP2 and LMP7 appear to be processed in "preproteasome" complexes before incorporation into active MCP (Frentzel et al., 1994). This processing involves conversion of these subunits from about M_r 30 000 to M_r 21 000 and M_r 23 000 for LMP2 and LMP7 (respectively). Here, however, RRC3 is present in nucleoplasmic MCP before its processing, which appears to occur when it associates with the NS. Such a posttranslational truncation would also be consistent with results with antisense oligonucleotides, since the pertinent mRNA appears to contain the N-terminal sequence from RRC3. One would not expect RRC3 antisense oligonucleotides, targeted to the 5′ initiation site of RRC3, to have any selective effects on the smaller M_r form, unless this sequence was also common to the two M_r forms. While alternative splicing of mRNAs could generate different proteins which share common N- and C-terminal regions, we consider this scenario considerably less likely than N-terminal truncation. First, we have not observed alternatively-spliced mRNAs on Northern analyses (Figure 7). Second, in metabolic ^{32}P-labeling studies, a minor amount of immunoprecipitable, larger M_r ^{32}P-labeled RRC3 was observed in nuclear preparations, but not in the cytosolic fraction (see below).

Another possibility, also considered unlikely, is that an internal initiation codon (amino acid 79) is utilized for translation of the nuclear form of RRC3. Such internal initiation may well be the case for other MCP subunits such as RING10 (Glynne et al., 1991). However, while the potential internal initiation codon within RRC3 would provide a strong consensus sequence (Kozak, 1989), internal initiation is not consistent with the "scanning" model for translation initiation (Kozak, 1989), and would eliminate the putative NLS (amino acids 50−53), although preserving potential tyrosine phosphorylation sites. One other unlikely possibility is that an in-frame CUG codon might be used for an alternative initiation site, as is involved in differential targeting which occurs with various growth factors (Kiefer et al., 1994; Prats et al., 1989); however, this would produce a protein of very similar size (differing by only 5 amino acids).

Nuclear RRC3 also differed from cytosolic RRC3 by showing tyrosine phosphorylation. Differential phosphorylation of nuclear RRC3 was observed using phosphotyrosine immunodetection, as well as with metabolic labeling of RRC3 with [^{32}P]orthophosphate followed by immunoprecipitation. In this regard, it has been speculated that phosphorylation of a conserved tyrosine residue, coupled with the presence of a NLS, could represent a mechanism for directing intranuclear translocation of certain MCP α subunits, including RRC3 (Tanaka et al., 1990b). While the

sites of tyrosine phosphorylation in nuclear RRC3 have not yet been identified, tyrosine 121 of RRC3 shows reasonable sequence similarities (at amino acids 78−150) to several receptor and viral proteins, which have tyrosine kinase activity and a conserved tyrosine autophosphorylation site (Tanaka et al., 1990b). Our results would appear to provide support for the idea that tyrosine phosphorylation may participate in nuclear import. Metabolic labeling experiments with [^{32}P]orthophosphate showed a minor phosphorylated form of RRC3 in nuclei, which migrated equivalently to the cytosolic form which was not phosphorylated, as well as the major form with M_r 24 000. We hypothesize that tyrosine phosphorylation of cytosolic RRC3 triggers rapid nuclear import, since no labeled M_r 28 000 form was observed in cytosol (Figure 2A). The M_r 28 000 form is present in the soluble nuclear fraction in MCP complexes (Figure 3), although whether it undergoes nuclear import as part of an MCP complex is not clear. This M_r 28 000 form then appears to be converted to the M_r 24 000 form, which is found in association with the NS (Figure 2B, lane 1). This truncation does not occur artifactually during NS preparation, since the M_r 24 000 form is also the major form observed with rapidly isolated nuclear preparations (Figure 2A). Our data also suggest that the phosphorylated M_r 28 000 RRC3 form is rapidly converted to the M_r 24 000 form.

The antisense oligonucleotide experiments produced a marked inhibition of cell growth, with differential affects on nuclear RRC3. RRC3 was completely eliminated in NS preparations, whereas cytosolic levels were only modestly reduced (by about 25%). Since RRC3 mRNA levels were dramatically reduced by the antisense treatments, this differential effect presumably involves differential turnover. Since cytoplasmic MCPs appear to be very stable with half-lives of 2 weeks (Tanaka & Ichihara, 1989), it is not surprising that there was a relatively small drop in cytoplasmic MCP. However, the data suggest that the NS form of RRC3 may have a much shorter apparent half-life. This could encompass changes in phosphorylation state and/or compartmentation. However, it seems pertinent to note that the marked growth-inhibiting effects of the antisense treatment appear to reflect effects upon the nuclear RRC3.

In spite of the dramatic reduction (80−100%) in NS RRC3 content, there was no alteration of the nuclear/NS chymotrypsin-like peptidase activities generally attributed to the catalytic β subunit(s), and total protease activities of the nuclear and NS fractions were also unaltered. Thus, the notion that nuclear translocation of RRC3 may somehow be coupled to translocation of an associated catalytic β subunit does not appear to be supported. RRC3 could, however, only participate in very specific proteolytic activities, which would presumably encompass multiple targets given the nonspecific cell cycle block. In this regard, there is evidence to suggest the importance of chymotrypsin-like proteases at multiple cell cycle stages (Brown et al., 1977; Clawson et al., 1992; Ponzio et al., 1990; Cunningham & Ho, 1975).

Another (albeit unlikely) possibility is that although the intranuclear transport of the β subunit may be blocked, the half-life of the β catalytic subunit may be substantially longer than that of RRC3. Quantitative RT/PCR and Northern analyses also showed no compensatory change in RRC9 levels (the other α subunit with a putative NLS), and we did not find any potential bipartite NLS (Robbins et al., 1991; Dingwall & Laskey, 1991) in other MCP subunits.

A wide variety of activities have been suggested for MCPs, although the scope of their catalytic functions remains unclear. MCPs have been categorized as serine proteases, based on DFP labeling and inactivation, despite the fact that the conserved serine protease catalytic triad (H-D-S) is not found in MCP subunits. Many MCP α subunits do, however, contain a conserved D residue (near amino acid 90), and two downstream conserved S residues (near amino acids 150, and 170) that could participate in catalysis. A conserved H is not found. In this regard, however, MCPs do contain a highly conserved Q (near amino acid 30), and it is conceivable that this Q has replaced the traditional H (a single nucleotide substitution) and is involved in forming an important structural motif for the α subunits, which are no longer catalytically active. It is also of interest to note that a number of proteins, generically referred to as "pseudoproteases" on the basis of serine protease sequence similarities, also show such an H to Q substitution. For example, human hepatocyte growth factor also has a Q (at amino acid 534) as an integral part of its homologous "catalytic" center (Michalopoulos & Zarnegar, 1992), as opposed to an H which is typically found in the active site of related proteases such as plasmin (Nakamura et al., 1989). Human hepatocyte growth factor does not, however, have chymotrypsin-like activity characteristic of the NS protease based on results of protease assays (data not shown). Other proteases, such as the yeast signal peptidase Imp2p (Nunnari et al., 1993), have similarly been classified as serine protease-like and have a highly conserved S residue (amino acid 70) as an integral part of their active site. Imp2P also has a D residue (amino acid 153) that may be involved in forming the catalytic site of these proteases. Again, however, no H residue appears to be required for their activity (Dalbey & von Heije, 1992). We therefore suggest that MCP α subunits may have evolved from serine proteases, and that their modifications (especially the H to Q substitution) may confer unique structural features which allow stable association into the higher-order structures characteristic of MCPs.

ACKNOWLEDGMENT

We thank Dr. Harriet Isom for generously providing NR4 cells, Dr. George DeMartino for providing rabbit antiserum raised against purified 20S bovine MCP, Nate Shaeffer for his technical assistance in flow cytometry analyses, and Dr. Judith Weisz and Gabriella Wolz for help with immunohistochemical studies.

REFERENCES

Aebi, U., Cohn, J., Buhle, L., & Gerace, L. (1986) *Nature 323*, 560.

Ausubel, F. M., Brent, R., Kingston, R. E., Moore, D. D., Seidman, J. G., Smith, J. A., & Struhl, K. (1994) in *Current protocols in molecular biology* (Ausubel, F. M., Brent, R., Kingston, R. E., Moore, D. D., Seidman, J. G., Smith, J. A., & Struhl, K., Eds.) pp 9.2−9.8, John Wiley and Sons Inc., New York.

Bey, F., Pereira, I., Coux, O., Viegas-Peguignot, E., Targa, F., Nothwang, H., Dutrillaux, B., & Scherrer, K. (1993) *Mol. Gen. Genet. 237*, 193.

Brown, R., Clark, R., Chiu, J., & Stubblefield, E. (1977) *Exp. Cell Res. 104*, 207.

Carter, K., Bowman, D., Carrington, W., Fogarty, K., McNeil, J., Fay, F., & Lawrence, J. (1993) *Science 259*, 1330.

Ciechanover, A., DiGiuseppe, J., Bercovich, B., Orian, A., Richter, J., Schwartz, A., & Brodeur, G. (1991) *Proc. Natl. Acad. Sci. U.S.A. 88*, 139.

Clawson, G., Wang, Y., Schwartz, A., & Hatem, C. (1990) *Cell Growth Differ. 1*, 559.
Clawson, G., Norbeck, L., Hatem, C., Rhodes, C., Amiri, P., McKerrow, J., Patierno, S., & Fiskum, G. (1992) *Cell Growth Differ. 3*, 827.
Clawson, G., Ren, L., & Isom, H. (1995) *Hepatology* (in press).
Cornish-Bowden, A. (1985) *Nucleic Acids Res. 13*, 3021.
Cunningham, D., & Ho, T. (1975) in *Proteases and Biological Control* (Reich, E., Rifkin, D., & Shaw, E., Eds.) pp 795–806, Cold Spring Harbor Laboratory, Cold Spring Harbor, NY.
Dahlmann, B., Kopp, F., Kuehn, L., Neidel, B., Pfeifer, G., Hegerl, R., & Baumeister, W. (1989) *FEBS Lett. 251*, 125.
Dahlmann, B., Kuehn, L., Grziwa, A., Zwickl, P., & Baumeister, W. (1992) *Eur. J. Biochem. 208*, 789.
Dalbey, R., & von Heijne, G. (1992) *Trends Biochem. Sci. 17*, 474.
Dingwall, C., & Laskey, R. A. (1991) *Trends Biochem. Sci. 16*, 478.
Driscoll, J., Brown, M., Finley, D., & Monaco, J. (1993) *Nature 365*, 262.
Frentzel, S., Pesold-Hurt, B., & Seeling, A. (1994) *J. Mol. Biol. 236*, 975.
Fruh, K., Gossen, M., Wang, K., Bujard, H., Peterson, P., & Yang, Y. (1994) *EMBO J. 13*, 3236.
Ghislain, M., Udvardy, A., & Mann, C. (1993) *Nature 366*, 358.
Glotzer, M., Murray, A., & Kirschner, M. (1991) *Nature 349*, 132.
Glynne, R., Powis, S., Beck, S., Kelley, A., Kerr, L., & Trowsdale, J. (1991) *Nature 353*, 357.
Gordon, C., McGurk, G., Dilion, P., Rosen, C., & Hastle, N. (1993) *Nature 366*, 355.
Heinemeyer, W., Gruhler, A., Mohrle, V., Mahe, Y., & Wolf, D. (1993) *J. Biol. Chem. 268*, 5115.
Heinemeyer, W., Trondle, N., Albrecht, G., & Wolf, D. H. (1994) *Biochemistry 33*, 12229.
Hershko, A., & Ciechanover, A. (1992) *Annu. Rev. Biochem. 61*, 761.
Hilt, W., Enenkel, C., Gruhler, A., Singer, T., & Wolf, D. H. (1993) *J. Biol. Chem. 268*, 3479.
Hoffman, L., & Rechsteiner, M. (1994) *J. Biol. Chem. 269*, 16890.
Hough, R., Pratt, G., & Rechsteiner, M. (1987) *J. Biol. Chem. 262*, 8303.
Isom, H. C., & Hu, J. (1993) in *In vitro toxicology: Tenth anniversary symposium of CAAT* (Goldberg, A. M., & Principe, M. L., Eds.) pp 79–90, Mary Ann Leibert, Inc., New York.
Isom, H., Woodworth, C., Meng, Y., Krieder, J., Miller, T., & Mengel, L. (1992) *Cancer Res. 52*, 940.
Kelley, A., Powis, S., Glynne, R., Radley, E., Beck, S., & Trowsdale, J. (1991) *Nature 353*, 667.
Kiefer, P., Acland, P., Pappin, D., Peters, G., & Dickson, C. (1994) *EMBO J. 13*, 4126.
Kozak, M. (1989) *J. Cell Biol. 108*, 229.
Kreutzer-Schmid, C., & Schmid, H. (1990) *FEBS Lett. 267*, 142.
Laemmli, U. (1970) *Nature 227*, 680.
Lawrence, J., Singer, R., & Marselle, L. (1989) *Cell 57*, 493.
Lowry, O., Rosebrough, N., Farr, A., & Randall, R. (1951) *J. Biol. Chem. 193*, 265.
Madsen, K., Fiskum, G., & Clawson, G. (1990) *Exp. Cell Res. 187*, 343.
Michalopoulos, G., & Zarnegar, R. (1992) *Hepatology 15*, 149.
Nakamura, T., Hishizawa, T., Hagiya, M., Seki, J. T., Shimonishi, M., Sugimura, A., Tashiro, K., & Shimiza, S. (1989) *Nature 342*, 440.
Newport, J., & Forbes, D. (1987) *Annu. Rev. Biochem. 56*, 535.
Nunnari, J., Fox, T., & Walter, P. (1993) *Science 262*, 1997.
Peters, J. M., Franke, W. W., & Kleinschmidt, J. A. (1994) *J. Biol. Chem. 269*, 7709.
Ponzio, G., Contreres, J., Debant, A., Auberger, P., Farahifar, D., & Rossi, B. (1990) *Growth Factors 4*, 37.
Prats, H., Kaghad, M., Prats, A. C., Klagbrun, M., Lelias, J. M., Liauzun, P., Chalon, P., Tauber, J. P., Amalric, F., Smith, J. A., & Caput, D. (1989) *Proc. Natl. Acad. Sci. U.S.A. 86*, 1836.
Puhler, G., Weinkauf, S., Bachmann, L., Muller, S., Engel, A., Hegerl, R., & Baumeister, W. (1992) *EMBO J. 11*, 1607.
Rechsteiner, M., Hoffman, L., & Dubiel, W. (1993) *J. Biol. Chem. 268*, 6065.
Renta, K., Getenberg, R., & Coffey, D. (1991) *Crit. Rev. Eukaryotic Gene Expression 1*, 355.
Richter-Ruoff, B., & Wolf, D. (1993) *FEBS Lett. 336*, 34
Robbins, J., Dilworth, S., Laskey, R., & Dingwall, C. (1991) *Cell 64*, 615.
Scheffner, M., Huibregtse, J., Viestra, R., & Howley, P. (1993) *Cell 75*, 495.
Seeling, A., Boes, B., & Kloetzel, P.-M. (1993) *Enzyme Protein 47*, 330.
Seufert, W., Futcher, B., & Jentsch, S. (1995) *Nature 373*, 78.
Sheetz, M., & Tager, H. (1988) *J. Biol. Chem. 263*, 19210.
Tamura, T., Shimbara, N., Aki, M., Ishida, N., Bey, F., Scherrer, K., Tanaka, K., & Ichihara, A. (1992) *J. Biochem. 112*, 530.
Tanaka, K., & Ichihara, A. (1989) *Biochem. Biophys. Res. Commun. 159*, 1309.
Tanaka, K., Kumatori, A., Il, K., & Ichihara, A. (1989) *J. Cell. Physiol. 139*, 34.
Tanaka, K., Fujiwara, T., Kumatori, A., Shin, S., Yoshimura, T., Ichihara, A., Tonkunaga, F., Aruga, R., Iwqanaga, S., Kakizoka, A., & Nakanishi, S. (1990a) *Biochemistry 29*, 3777.
Tanaka, K., Yoshimura, T., Fujiwara, T., Kumatori, A., & Ichihara, A. (1990b) *FEBS Lett. 271*, 41.
Tokes, Z., & Clawson, G. (1989) *J. Biol. Chem. 264*, 15059.
Treier, M., Straszewski, L., & Bohmann, D. (1994) *Cell 78*, 787.
Tsukhara, T., Ishiura, S., & Sugita, H. (1988) *Eur. J. Biochem. 177*, 261.
Weitman, J., & Etlinger, J. (1992) *J. Biol. Chem. 267*, 6977.
Woodworth, C., Secott, T., & Isom, H. (1986) *Cancer Res. 46*, 4018.
Xing, Y., Johnson, C., Dobner, P., & Lawrence, J. (1993) *Science 259*, 1326.
Zwickl, P., Grziwa, A., Puhler, G., Dahlmann, J., Lottspeich, R., & Baumeister, W. (1992) *Biochemistry 31*, 96.

BI950256V